CrystEngComm

Accepted Manuscript

ROYAL SOCIETY OF CHEMISTRY

www.rsc.org/crystengcomm

High pressure synthesis and characterization of diamond from an Mg-Si-C system

Y. N. Palyanov,[*a] I. N. Kupriyanov,[ab] Y. M. Borzdov,[a] and Y. V. Bataleva[a]

[a] *Sobolev Institute of Geology and Mineralogy, Siberian Branch of Russian Academy of Sciences, Koptyug ave., 3, 630090, Novosibirsk, Russia*

[b] *Novosibirsk State University, 630090, Novosibirsk, Russia*

* Corresponding author.

Email: palyanov@igm.nsc.ru

Tel./Fax: +7-383-3307501

Abstract

Diamond crystallization in the Mg-Si-C system has been studied at high pressure high temperature conditions of 7 GPa and 1500-1900 ºC. The features of nucleation and growth of diamond from the carbon solution in the Mg-Si melt are established. The degree of the graphite-to-diamond transformation is found to depend significantly on the crystallization temperature. As opposed to the pure Mg-C system where the cubic morphology dominates, the octahedron with the antiskeletal structure of faces is the dominant form of growth in the Mg-Si-C system over the entire temperature range. The possibility of epitaxial growth of silicon carbide tetrahedral crystals on diamond upon their co-crystallization was noted. Synthesized diamond are found to contain optically active silicon-vacancy (Si-V) centers and inactive substituional silicon defects, giving rise to the 1.68 eV system in the photoluminescence spectra and an absorption peak at 1338 cm^{-1} in the infrared absorption spectra, respectively.

Introduction

Diamond possessing a range of unique physical properties has been attracting considerable attention in modern fundamental and application driven research. Currently, one of the most exciting and rapidly developing areas in the diamond research is connected with the engineering of point defects, commonly termed as color centers, in diamond with specific optical, electronic and magnetic properties. It has been demonstrated that color centers in diamond are a very promising platform for the emerging technologies of quantum information processing,[1,2] electromagnetic field sensing,[2,3] and bio-imaging.[2,4] Until recently, the major efforts have been focused on the nitrogen-vacancy (N-V) centers in diamond. A number of impressive results such as demonstration of quantum entanglement of spin states[5] and detection of weak magnetic fields with nano-scale resolution[6] were achieved with the N-V centers. During the past few years several important findings[7-11] have been made demonstrating that the well-known 1.68-eV silicon-vacancy (Si-V) center in diamond could be a better alternative to the N-V centers for many applications. One of the advantages of the 1.68-eV Si-V center is that electronic transitions at this center are very weakly coupled to lattice vibrations resulting in the predominance of the zero-phonon line (ZPL) emission/absorption even in the room temperature spectra.[12]

The overwhelming majority of studies devoted to the Si-V centers in diamond have been concerned with diamonds produced by the chemical vapor deposition (CVD), for which silicon is known to be a characteristic impurity. Unless special measures are taken, unintentional doping of CVD diamonds with Si is frequently observed being a consequence of plasma etching of silicon containing reactor components.[13,14] Recently considerable progress has been made in growing CVD diamonds with controlled content of silicon impurities.[8,15-17] Several methods were demonstrated to be efficient for synthesis of nano- and micro-diamonds with high concentrations of the Si-V centers. These include growth on silicon substrates pretreated with Ni nanoparticles[16] and, more commonly, addition of silane (SiH_4) to the feed-gas mixture.[17,18] It was however found that high concentrations of silane in the feed-gas mixture had detrimental effects on the quality of synthesized diamonds.[17]

Another approach potentially suitable for production of diamond crystals doped with silicon is the growth at high pressure high temperature (HPHT) conditions using Si containing solvent-catalysts. Clark et al.[19] and Sittas et al.[20] demonstrated growth of diamond crystals with Si-V centers using HPHT technique with conventional metal solvent-catalysts and silicon additives. The high crystalline quality of the produced Si doped diamonds enabled the study of the fine structure of the zero-phonon transitions at the 1.68-eV center and revealing the line splitting due to Si isotopes.[19] To the best of our knowledge no detailed studies on the growth and

properties of Si doped HPHT diamonds have been reported over the last almost 20 years. Very recently a few works appeared reporting HPHT synthesis of diamond with intense photoluminescence from the 1.68 eV Si-V centers using a mixture of hydrocarbon, fluorocarbon and organosilicon compounds[21] and Mg-C system.[22,23] It is interesting that in the latter case silicon was not deliberately added to the growth systems but contained as a trace impurity in the starting reagents, indicating high doping efficiency for the magnesium based systems. However, there is still no information on diamond synthesis from Si-rich environments at HPHT conditions. Despite silicon is one of the few elements able to incorporate in the diamond lattice during the growth, no detailed investigations into its effect on HPHT diamond crystallization process have been reported yet. This is in contrast with other important impurities in diamond, such as nitrogen, boron and hydrogen, whose influence on both growth and properties of diamond has been extensively studied.[24-28]

In view of the very promising properties of the Si-V centers in diamond, lack of detailed information about Si effects on diamond growth, and a significant potential of HPHT techniques for growing high-quality diamond crystals, we have undertaken a detailed instigation into the diamond crystallization process in the Mg-Si-C system. The choice of the Mg-based system is substantiated by our recent results obtained for the Mg-C system.[23] It was found that diamond crystallization in this system takes place over a broad range of temperatures, shows very high growth rates and produces diamond crystals with specific morphology and internal structure. The Mg-based systems are relatively poor studied as the diamond forming media but demonstrating a number of interesting features deserves further detailed investigations. In the present study, experiments were performed with a fixed $Mg_{0.8}Si_{0.2}$-C composition at a pressure of 7 GPa, temperatures in the range of 1500-1900 °C and reaction times from 10 min to 20 h. The produced diamond crystals were characterized using a set optical spectroscopy techniques.

Experimental section

The experiments on diamond crystallization in the Mg-Si-C system were conducted at a pressure of 7 GPa and temperatures in the range of 1500-1900 ºC using a split sphere multi-anvil high pressure apparatus.[24] Taking into account experimental data on the kinetics of diamond crystallization in the Mg-C system,[23] the duration of the experiments was varied from 10 min to 20 h depending on the temperature. A high-pressure cell in the form of 19×19×22 mm tetragonal prism,[29] was used in the experiments. Pressure was calibrated at room temperature by the pressure-induced phase transitions of Bi (2.55 GPa) and PbSe (4.0 and 6.8 GPa), and corrected at high temperatures by referencing to the graphite-diamond equilibrium line.[30] Temperature was measured in each experiment using a $PtRh_6/PtRh_{30}$ thermocouple. The thermocouple was placed

inside the graphite heater so that its junction was close to the crystallization capsule. Details of the calibration of the P-T parameters have been presented elsewhere.[31] The starting materials were a graphite rod (99.99% purity), Mg (99.9% purity), Si (99.99% purity), and cuboctahedral synthetic diamonds (*ca.* 0.5 mm) as the seed crystals. The graphite rod was machined into thick-walled capsules 6.9 mm in diameter and 6.5 mm high. A mixture of powders of the $Mg_{0.8}Si_{0.2}$ composition and four seed crystals were placed into the center of the graphite capsule. The graphite capsule was enveloped from all sides with a 0.1 mm thick molybdenum foil and insulated from the graphite heater with a MgO/CsCl insulating sleeve. After experiments, the products were dissolved in diluted nitric acid. The degree of the graphite-to-diamond conversion, α, which is defined as $\alpha=M_{Dm}/(M_{Dm} + M_{Gr})\times100$, where M_{Dm} is the mass of synthesized diamond and M_{Gr} is the mass of residual graphite[32] was determined for each growth run. The recovered diamond crystals and associated phases were studied using an Axio Imager Z2m optical microscope and a LEO 420 scanning electron microscope (SEM) equipped with an energy dispersive spectroscopy (EDS) attachment. Spectroscopic characterization of diamond crystals was performed by means of infrared (IR) absorption, photoluminescence (PL) and Raman scattering. IR spectra were measured using a Bruker Vertex 70 Fourier transform infrared (FTIR) spectrometer fitted with a Hyperion 2000 microscope. To convert the recorded spectra into the absorption coefficient units each spectrum was fitted to the standard infrared spectrum of type IIa diamond so that to obtain the best fit of the intrinsic two-phonon absorption bands (2700-1700 cm^{-1}). Raman/PL spectra were measured using a Horiba J.Y. LabRAM HR800 spectrometer with a 523 nm solid state laser as the excitation source. For the low temperature measurements a Linkam FTIR600 heating/freezing stage was used.

Results

Diamond crystallization

The conditions and results of the experiments on diamond crystallization in the $Mg_{0.8}$-$Si_{0.2}$-C system are summarized in Table 1. The choice of the experimental duration at different temperatures was made with the account of the diamond crystallization kinetics in the Mg-C system studied over the same temperature range.[23] At 1900 ºC, short experiments with run times of 20 and 10 min (runs 1761/1 and 1767/2) were conducted, but the degree of the graphite-to-diamond transformation was very high reaching 100 and 90 %, respectively. In both experiments diamond was predominantly represented by crystal blocks sizing up to 1.4 mm and showing some faceting elements and cleavage surfaces. Major {111} faces with the stepped structure and minor {100} faces were present on the blocks as the faceting elements. Octahedral diamond crystals, sometimes with the {100} faces, twins, and intergrowth aggregates were found in the

central part of the capsule (Fig. 1a-c). These crystals were from 100 to 500 μm in size and varied in color from colorless to light brown. Tetrahedral silicon carbide crystals of 1 to 15 μm in size grown on the diamond surface were revealed using an electron microscope. The cubic 3C-SiC phase (moissanite) of the crystallized silicon carbide was confirmed by the Raman measurements. The seed crystals were partially dissolved and then regenerated in the stability region of the octahedral growth form.

At 1800 ºC, the graphite capsule was completely transformed into a large-block diamond aggregate after 2 h (run 1320/3). Most of the crystals were cleaved along {111}. Examination of the individual blocks, whose size reached 2 mm, showed that the {111} faces with the stepped structure (Fig. 1d-f) dominated in the crystal faceting. The produced crystals were mainly colorless or gray, and had sometimes areas with brown coloration. In the central part of the capsule, plate-like crystals bound by the {111} faces with the pronounced stepped structure were found. The seed diamond crystals were strongly dissolved and then regenerated mainly by the {111} faces. In addition to diamond, tetrahedral silicon carbide crystals up to 20 μm in size were found in the central part of the capsule (Fig. 2a-c). Silicon carbide tetrahedrons were grown on the diamond crystals and sometimes entrapped by growing diamonds as inclusions. Similar results were obtained in the experiment 872/7 with a run time of 30 min. In this case, the degree of the graphite-to-diamond transformation was approximately 90 %.

At the temperature of 1700 ºC (runs 875/7, 864/7 and 859/7), crystallized diamonds were also represented by polycrystalline aggregate blocks. The crystals were usually non-uniform in color and had colorless, gray and brown parts. Similarly to higher temperatures, the diamond morphology was primarily determined by the {111} faces, while the {100} faces were slightly developed. As the experimental duration was increased from 30 min to 2 h, the degree of the graphite-to-diamond transformation increased from 50 to 70%. In a 4-h experiment, approximately 95% of the starting graphite capsule was converted to diamond. In all the experiments performed at 1700 ºC, silicon carbide crystals and small amounts of metastable graphite were found in the central part of the capsules.

At 1600 ºC the degree of the graphite-to-diamond conversion was approximately 10 and 35% after 4 and 10 h, respectively. Crystallized diamonds were in the form of relatively large polycrystalline blocks up to 1.5 mm in size. The crystals appeared black and opaque, but in thin sections were transparent and exhibited dark brown or reddish brown coloration. The morphology of the crystals was determined by the major {111} faces, minor {100} faces were present sometimes. A large number of silicon carbide crystals having mainly tetrahedral morphology as well as lamellar crystals of metastable graphite were found in the central part of the capsules. At 1500 ºC and a run time of 20 h, very small (up to 5 μm) diamond crystals were

detected in the run products. The seed diamond crystals were significantly dissolved and showed no elements of growth.

Spectroscopic characterization

Spectroscopic characterization of the diamond crystals produced in the Mg-Si-C system was performed using infrared absorption, photoluminescence and Raman scattering techniques. As described in the preceding section, diamonds produced at 1600 °C were mostly black and opaque, but in thin sections showed intense brown or reddish brown coloration. This coloration appeared similar to that observed for diamonds produced in the pure Mg-C system.[23] Indeed, infrared absorption and Raman spectra recorded for these diamonds were found to be in general similar to those measured for diamonds from the Mg-C system. A continuous absorption steadily increasing in strength toward higher wavenumbers and weak absorption features related to boron impurities were present in the IR spectra (Fig. 3a). In the Raman spectra a band peaking at about 1480 cm^{-1} along with the diamond Raman peak at 1332 cm^{-1} were detected (Fig. 4a). Both the continuous absorption and the 1480 cm^{-1} band were tentatively assigned to defects involving π-bonded carbon atoms, responsible for the brown coloration.[23] In the photoluminescence spectra a peak at 1.682 eV due to the Si-V centers was found for all samples examined, though its intensity for a given sample vary significantly from one point to another. In addition a relatively weak peak at 1.722 eV was present in the PL spectra.

Diamond crystals with strong brown coloration were less abundant in the products of experiments performed at 1700-1900 °C. In addition, for these higher temperatures it was possible to discern diamonds crystallized in the central part of the capsules within the carbon-saturated Mg-Si melt and diamonds, which crystallized at the melt-graphite interface and grew towards the graphite capsule. Infrared absorption measurements (Fig. 3b-c) revealed that the synthesized diamonds typically contained boron impurities even though boron was not deliberately added to the growth system, but was present as a trace impurity in the starting reagents. Similar observation was made previously for diamonds produced in the nominally pure Mg-C system.[23] The concentration of uncompensated boron acceptors was calculated using the relation $[B^0](ppm)=0.55\times10^{-3}\times I(2800\ cm^{-1})$, where $I(2800\ cm^{-1})$ is the integrated absorption of the boron-related peak at 2800 cm^{-1} (expressed in cm^{-2} units).[33] The calculations showed that diamonds that grew towards graphite typically contained boron impurities in concentrations from 0.5 to 1.5 ppm with a tendency that crystals produced at higher temperatures had on average higher boron concentrations. On the other hand, diamonds crystallized in the central part of the capsules contain still noticeable but much lower boron concentrations of order of 0.1 ppm and less. An interesting feature of these diamonds is the presence of a sharp absorption peak in the IR

spectra located at 1338 cm^{-1} (Fig. 5), *i.e.* at wavenumbers slightly higher than that of the highest energy zone-center phonons of diamond (1332 cm^{-1}). Absorption strength of this peak varied from about 0.5 to 5-6 cm^{-1} for diamonds synthesized at 1700 and 1900 °C, respectively. Possible nature of the 1338 cm^{-1} peak will be discussed below. Raman spectra measured for the crystals produced at 1700-1900 °C were dominated by the diamond Raman peak at 1332 cm^{-1} (Fig. 4b). No bands due graphitic or π-bonded carbon defects were found even for crystals showing brown coloration. Occasionally peaks due to SiC inclusions were also present in the Raman spectra (Fig. 4c). Photoluminescence spectra recorded for diamond crystals synthesized at 1700, 1800 and 1900 °C were in general similar and dominated by the emission from the 1.68-eV silicon-vacancy (Si-V) center (Fig. 6). The intensity of the 1.682 eV peak, normalized to the intensity of the diamond Raman line, showed a tendency to increase with crystallization temperature. For a given temperature, photoluminescence from the 1.68-eV center was more intense for crystals extracted from the central part of the capsules. In addition to the 1.68 eV system a narrow peak located at 1.722 eV was present in the PL spectra of most of the crystals examined. As a rule this peak had much lower intensity than that of the 1.682 eV line. However, in a few cases PL spectra as shown in Fig. 7 exhibited peaks at 1.682 and 1.722 eV of comparable intensity.

Discussion

The obtained experimental results enable us to consider the features diamond crystallization in the Mg-Si-C system in comparison with the Mg-C system studied under the same *P-T* conditions and using the same assemblies for the high-pressure cells and crystallization capsules.[23] Figure 8 shows degree of the graphite-to-diamond transformation (α) in the Mg-C and $Mg_{0.8}$-$Si_{0.2}$-C systems as a function of the run time at different temperatures in the range of 1500−1900 ºC. At 1500 ºC and a run time of 20 h, only minute diamonds were synthesized in both systems, with the transformation degree α being much smaller than unity. Thus, the catalytic abilities of these systems for the conversion of graphite to diamond are comparable at the lowest temperature. At 1600 and 1700 ºC, the degree of the graphite-to-diamond transformation in the Mg-Si-C system drastically increases relative to the Mg-C system. Obviously, at these temperatures, the duration of the induction period preceding diamond nucleation is significantly reduced, and the growth rate of diamond is likely to increase. At temperatures of 1800 and 1900 ºC, the tendency toward an increase in α with addition of silicon to the Mg-C system remains, but it becomes less obvious because of the very high rates of the graphite-to-diamond transformation. It is possible that one of the main causes for an increase in α in the Mg-Si-C system relative to the Mg-C system is an increase in the solubility of carbon in a binary melt comprising two carbide-forming elements Mg and Si. Unlike the Mg-C system,

where diamond crystallizes predominantly with the cubic morphology, the dominant growth form of diamond in the Mg-Si-C system is octahedron. However, plane-faced octahedrons (Fig. 1a) are extremely rare, and the majority of the crystals have {111} faces with the stepped structure. The macrosteps on the {111} surfaces propagate in the [221] directions. Generators of the growth macrolayers are located on the {111} faces, but not at the vertices and edges of the crystals. They can be single, being usually located in the central part of a face, or multiple. In the former case, crystals with the convex stepped octahedral faces (Fig. 1f) are formed, and, in the latter case, crystals with the polycentric structure of faces are produced (Figs. 1d, 9a). The macrolayers or macrosteps are formed by accumulation of serrate or curvilinear microlayers (Fig. 1d,e). During growth, new layers are formed before several previous layers reach the face edge or the macrostep boundary. Growth layers usually form macrosteps built up of the {111} faces whose combination creates on crystals a lot of re-entrant corners and striations in the [110] direction. In some parts of the {111} faces, pyramids built up of the {111}, {hkk} (tetragon-trioctahedron), {100}, and {110} faces (Figs. 2b, 9) or solely {111} faces (Fig. 1d-f) are formed. The established morphological features allow us to consider the produced diamonds as a sort of antiskeletal crystals. The formation of similar antiskeletal diamond crystals, which were previously obtained in the conventional metal-carbon systems with addition of H_2O impurities, was considered from the viewpoint of the impurity adsorption influence.[34]

As described above, silicon carbide (SiC) is observed in the products of all experiments in the $Mg_{0.8}$-$Si_{0.2}$-C system. Silicon carbide forms tetrahedral crystals, polysynthetic twins along (111), and irregular aggregates (Figs. 2, 10a,b). Visualization of SiC crystals in SEM is most preferable in the backscattered electrons mode. Due to the higher atomic weight of silicon relative to that of carbon, SiC crystals look much brighter than diamond in the SEM images. Our results indicate that silicon carbide does not form upon quenching but crystallizes together with diamond in the course of experiments. This is evidenced by the intergrowth between SiC and diamond (Figs. 2, 10a,b) as well as inclusions of faceted SiC crystals inside diamond. Consequently, we can infer that the solubility of silicon in the Mg-Si-C system is less than 20 wt.% over the entire investigated range of temperatures. Although most of the silicon carbide crystals are randomly located on diamond crystals, some of them, as shown in Fig. 2, demonstrate regular orientation. The faces and edges of the silicon carbide tetrahedrons are parallel to the faces and edges of the diamond octahedron. This suggests epitaxial relationship between silicon carbide and diamond. In the experiment 872/7, submicron microspheres were found on diamond crystals (Fig. 10c). EDS analysis shows that the chemical composition of the microspheres is $(Si_{0.75}Mg_{0.25})C_2$ and does not vary from samples to sample. We suppose that these microspheres correspond to mixed silicon-magnesium carbide. As can it be seen from Fig.

10b,c, the SiC crystals and $(Si_{0.75}Mg_{0.25})C_2$ spheres precipitated on the diamond crystal surfaces act as stoppers preventing the propagation of the growth macrosteps and ultimately resulting in the specific diamond morphology. Based on the results of analysis of the obtained crystals and taking into account experimental data on the formation of antiskeletal diamond crystals,[34,35] we can suggest that diamond growth in the Mg-Si-C system takes place under the impurity adsorption influence. Silicon or silicon-carbide clusters may be considered as the impurities adsorbing on the growing diamond surfaces and inhibiting the propagation of the growth layers and macrosteps, while silicon carbide microcrystals and magnesium-silicon carbide microspheres may be considered as the stoppers blocking the growth macrosteps.

Let us now briefly discuss the results of the spectroscopic characterization of diamond crystals produced in the Mg-Si-C system. The 1.68-eV silicon-vacancy center is observed in photoluminescence spectra of all crystals examined with a tendency that crystals produced at higher temperatures show higher intensities of the 1.682 eV peak. For diamonds produced at 1700-1900 °C infrared absorption measurements reveal an absorption peak at 1338 cm^{-1} which also increase in strength with temperature. We found several publications[36-39] mentioning that for CVD diamonds deliberately doped with silicon an absorption peak at around 1338 cm^{-1} was observed in IR spectra. Unfortunately, in all these works either private communications or publicly inaccessible conference materials were given as the references to this finding, so that no details of the measured spectra and Si doping level are available for comparison. As suggested by theoretical calculations reported by Goss et al.,[36] the 1338 cm^{-1} peak can be related to a localized mode originating due to the strain surrounding substitutional silicon atoms in the diamond lattice. Our results corroborate the unpublished data for the occurrence of the silicon related IR absorption in Si doped diamond. Further challenging task is to relate the intensity of the 1338 cm^{-1} peak to the concentration of substitutional silicon impurities. It is worth noting that for diamond crystals synthesized in the nominally pure Mg-C system,[23] which also exhibited silicon-related centers in PL spectra, no absorption peak at 1338 cm^{-1} was found in the IR spectra, which can be reasonably explained by lower concentrations of silicon impurities in these diamonds.

In addition to the 1.68 eV Si-V center PL spectra of diamonds synthesized in the Mg-Si-C system frequently exhibit an optical system with a zero-phonon line (ZPL) at 1.722 eV. Phonon sideband associated with the 1.722 eV ZPL is relatively weak and masked by the 1.68 eV system. The origin of the observed 1.722 eV optical center in not clear at the moment. It is worth noting that a luminescence band centered at around 1.72 eV was reported in a number of previous works on CVD diamonds and attributed to vacancy clusters or graphitic defects.[18,40] However, in all these works the 1.72 eV luminescence feature appeared in the spectra as a broad

band rather than a narrow peak. Furthermore, the narrowness and fixed position of the observed 1.722 eV peak suggest that the corresponding defect is unlikely an extended cluster, but posses a well defined atomic structure.

Conclusions

Diamond crystallization in the Mg-Si-C system has been implemented at 7 GPa over the broad temperature range from 1500 to 1900 ºC. Nucleation and growth of diamond are found to occur from a carbon solution in the Mg-Si melt. The degree of the graphite-to-diamond conversion in the Mg-Si-C system considerably increases with temperature and is significantly higher than that found for the pure Mg-C system in the 1600-1900 ºC interval. An excess of silicon in the system leads to co-crystallization of diamond, silicon carbide and a complex carbide of the $(Si_{0.75}Mg_{0.25})C_2$ composition. Regular oriented growth of silicon carbide tetrahedral crystals on the octahedral faces of diamond is found. Unlike the Mg-C system, where the cubic morphology is the stable growth form irrespective of *P-T* conditions, the dominant growth form of diamond in the Mg-Si-C system is octahedron, which is stable over the entire temperature range studied (1500 to 1900 ºC). The {100}, {hkk}, and {110} faces are found to be minor faces. Diamond growth takes place by the tangential mechanism. Single or multiple sources of growth layers are located on the {111} faces, and the growth macrosteps propagate along the [221] directions. The dominant antiskeletal structure of the {111} faces of the synthesized diamond crystals allows us to suggest that they are formed under conditions of the adsorption influence of impurities. Silicon or silicon carbide clusters may act as the adsorbing impurities, while silicon carbide microcrystals or magnesium-silicon carbide microspheres may be responsible for blocking the propagation of the growth macrosteps. Synthesized diamond are found to contain optically active silicon-vacancy centers and inactive substituional silicon defects, giving rise to the 1.68 eV system in the PL spectra and an absorption peak at 1338 cm^{-1} in the IR spectra, respectively. To summarize, this study has provided novel experimental data on the effect of silicon on the growth, morphology and optical characteristics of diamond. We have established that the silicon addition to the Mg-C system leads to an increase in the degree of the graphite-to-diamond transformation, changes diamond crystal morphology from the cube to octahedron and results in new silicon related centers in diamond.

Acknowledgements

This work was supported by the Russian Science Foundation under Grant No. 14-27-00054. Alexander Khohryakov and Andrew Moskalev are thanked for their assistance in the study and manuscript preparation, respectively.

Notes and references

1 J. Wrachtrup and F. Jelezko, *J. Phys. Condens. Matter*, 2006, **18**, S807-S824.

2. *Quantum Information Processing with Diamond*, ed. S. Prawer and I. Aharonovich, Woodhead Publishing, 2014, 330 pp.

3 J. M. Taylor, P. Cappellaro, L. Childress, L. Jiang, D. Budker, P. R. Hemmer, A. Yacoby, R. Walsworth and M. D. Lukin, *Nature Phys*., 2008, **4**, 810-816.

4 A. S. Barnard, *Analyst*, 2009, **134**, 1751-1764.

5 F. Dolde, I. Jakobi, B. Naydenov, N. Zhao, S. Pezzagna, C. Trautmann, J. Meijer, P. Neumann, F. Jelezko and J. Wrachtrup, *Nature Phys*., 2013, **9**, 139-143.

6 P. Maletinsky, S. Hong, M. S. Grinolds, B. Hausmann, M. D. Lukin, R. L. Walsworth, M. Loncar and A. Yacoby, *Nature Nanotech*., 2012, **7**, 320-324.

7 I. I. Vlasov, A. S. Barnard, V. G. Ralchenko, O. I. Lebedev, M. V. Kanzyuba, A. V. Saveliev, V. I. Konov and E. Goovaerts, *Adv. Mater*. 2009, **21**, 808–812.

8 E. Neu, D. Steinmetz, J. Riedrich-Möller, S. Gsell, M. Fischer, C. Schreck and M. Becher, *New J. Phys*., 2011, **13**, 025012.

9 T. Muller, C. Hepp, B. Pingault, E. Neu, S. Gsell, M. Schreck, H. Sternschulte, D. Steinmuller-Nethl, C. Becher and M. Atature, *Nat. Comm*., 2014, **5**, 3328.

10 L. J. Rogers, K. D. Jahnke, T. Teraji, L. Marseglia, C. Muller, B. Naydenov, H. Schauffert, C. Kranz, J. Isoya, L. P. McGuinness and F. Jelezko, *Nat. Comm*., 2014, **5**, 4739.

11 J. Song, H. Li, F. Lin, L. Wang, H. Wu and Y. Yang, *CrystEngComm*, 2014, **16**, 8356-8362.

12 K. D. Jahnke, A. Sipahigil, J. M. Binder. M. W. Doherty, M. Metsch, L. J. Rogers, N. B. Manson, M. D. Lukin and F. Jelezko, *New J. Phys*., 2015, **17**, 043011.

13 J. Barjon, E. Rzepka, F. Jomard, J. M. Laroche, D. Ballutaud, T. Kociniewski and J. Chevallier, *Phys. Status Solidi A*, 2005, **202**, 2177-2181.

14 J. Achard, A. Tallaire, R. Sussmann, F. Silva and A. Gicquel, *J. Cryst. Growth*, 2005, **284**, 396-405.

15 A. Tallaire, J. Achard, F. Silva, O. Brinza and A. Gicquel, *Comptes Rendus Physique*, 2013, **14**, 169-184.

16 I. Cianchetta, M. Tomellini, E. Tamburri, S. Gay, D. Porchetta, M. L. Terranova and S. Orlanducci. *J. Mater. Chem. C*, 2014, **2**, 9666–9673.

17 S. A. Grudinkin, N. A. Feoktistov, A. V. Medvedev, K. V. Bogdanov, A. V. Baranov, A. Y. Vul' and V. G. Golubev, *J. Phys. D: Appl. Phys*., 2012, **45**, 062001.

18 D. V. Musale, S. R. Sainkar and S. T. Kshirsagar, *Diamond Rel. Mater*., 2002, **11**, 75-86.

19 C. D. Clark, H. Kanda, I. Kiflawi and G. Sittas, *Phys. Rev. B*, 1995, **51**, 16681-16688.

20 G. Sittas, H. Kanda, I. Kiflawi and P. M. Spear, *Diam. Relat. Mater.*, 1996, **5**, 866-869.

21 V. A. Davydov, A. V. Rakhmanina, S. G. Lyapin, I. D. Ilichev, K. N. Boldyrev, A. A. Shiryaev and V. N. Agafonov, *JETP Letters*, 2014, **99**, 585-589.

22 T. V. Kovalenko and S. A. Ivakhnenko, *J. Superhard Mater*., 2013, **35**, 131-136.

23 Y. N. Palyanov, Y. M. Borzdov, I. N. Kupriyanov, A. F. Khokhryakov and D.V. Nechaev, *CrystEngComm*, 2015, **17**, 4928-4936.

24 Yu. N. Palyanov, Yu. M. Borzdov, A. F. Khokhryakov, I. N. Kupriyanov and A. G. Sokol, *Cryst. Growth Des*., 2010, **10**, 3169-3175.

25 Y. Palyanov, I. Kupriyanov, A. Khokhryakov and V. Ralchenko, in *Handbook of Crystal Growth*, ed. P. Rudolph, Elsevier, Amsterdam, 2nd edn, 2015, ch. 17, vol. 2a 2015, pp. 671–713.

26 S. Sun, X. Jia, B. Yan, F. Wang, N. Chen, Y. Li and H. Ma, *CrystEngComm*, 2014, **16**, 2290-2297.

27 Y. Li, X. Jia, H. Ma, J. Zhang, F. Wang, N. Chen and Y. Feng, *CrystEngComm*, 2014,16, 7547-7551

28 V. D. Blank, M. S. Kuznetsov, S. A. Nosukhin, S. A. Terentiev and V. N. Denisov, *Diamond Relat. Mater.,* 2007, **16**, 800-804.

29 Y. N. Palyanov, Y. M. Borzdov, I. N. Kupriyanov, Y. V. Bataleva, A. F. Khokhryakov and A. G. Sokol, *Cryst. Growth Des*., 2015, **15**, 2539-2544.

30 C. S. Kennedy and G. Kennedy, *J. Geophys. Res*., 1976, **81**, 2467-2470.

31 A. G. Sokol, Y. M. Borzdov, Y. N. Palyanov and A. F. Khokhryakov, *High Press. Res*., 2015, **35**, 39-147.

32 Yu. N. Palyanov and A.G. Sokol, *Lithos*, 2009, **112S**, 690-700.

33 A.T. Collins and A.W.S. Williams, *J. Phys. C: Solid State Phys*. 4 (1971) 1789

34 Yu. N. Palyanov, A. F. Khokhryakov, Yu. M. Borzdov and I. N. Kupriyanov, *Cryst. Growth Des.*, 2013, **13**, 5411-5419.

35 Yu. N. Palyanov, Yu. M. Borzdov, I. N. Kupriyanov and A. F. Khokhryakov, *Cryst. Growth Des*., 2012, **11**, 5571-5578.

36 J. P. Goss, P. R. Briddon, and M. J. Shaw, *Phys. Rev. B*, 2007, **76**, 075204.

37 C. M. Breeding and W. Wang, *Diam. Relat. Mater*., 2008, **17**, 1335-1344.

38 A. M. Edmonds, Ph.D. Thesis, University of Warwick, 2008.

39 U. F. S. D'Haenens-Johansson, Ph.D. Thesis, University of Warwick, 2011.

40 S. Dannefaer, W. Zhu, T. Bretagnon and D. Kerr, *Phys. Rev. B*, 1996, **53**, 1979-1984.

Table 1. Experimental results

Run No.	P, GPa	T,°C	Time, h	Diamond growth on seeds	Diamond nucleation	α,(%) Gr→Dm transformation
1761/1	7	1900	0.33	+	+	100
1767/2	7	1900	0.16	+	+	90
872/7	7	1800	0.5	+	+	90
1320/3	7	1800	2	+	+	100
875/7	7	1700	0.5	+	+	50
864/7	7	1700	2	+	+	70
859/7	7	1700	4	+	+	95
858/7	7	1600	4	+	+	10
1782/1	7	1600	10	+	+	35
1744/2	7	1500	20	-	+	<<1

"+" – was observed; "-" – was not observed. α is the degree of the graphite-to-diamond transformation, $\alpha = M_{Dm}/(M_{Dm}+ M_{Gr})100$, where M_{Dm} is the mass of obtained diamond and M_{Gr} is the mass of residual graphite. Dm - diamond, Gr - graphite.

Figure captions

Figure 1. SEM micrographs of diamond produced in the Mg-Si-C system: (a) a flat-face octahedral diamond crystal; (b) an octahedron with minor {100} faces; (c) a contact twin of diamond octahedrons with the stepped structure of the faces; (d) an octahedron with the polycentric structure of the faces; (c) pyramidal features and growth microlayers on the {111} face (an enlarged fragment of (d)); (f) an octahedron with convex stepped {111} faces.

Figure 2. SEM micrographs of co-crystallized diamond and silicon carbide: (a) general view; (b, c) fragments of the diamond surface with regularly oriented tetrahedral SiC crystals. The micrographs are taken in the backscattered electrons mode.

Figure 3. Typical infrared absorption spectra of diamond crystals synthesized in the Mg-Si-C systems at different temperatures: (a) 1600 °C, (b) 1800 °C, (c, e) 1900 °C, (d) 1700 °C. Spectra (b, c) and (d, e) were recorded for diamonds recovered from the central and outer parts of the capsules, respectively. The spectra are displaced vertically for clarity.

Figure 4. Representative Raman spectra measured for diamond crystals synthesized in the Mg-Si-C system at (a) 1600 °C and (b) 1700-1900 °C. Spectrum (c) corresponds to SiC inclusions in diamond.

Figure 5. Infrared spectra demonstrating the 1338 cm^{-1} absorption peak. The spectra were recorded for diamonds synthesized in the Mg-Si-C system at (a) 1700 °C, (b, c) 1800 °C and (d, e) 1900 °C. The spectra are displaced vertically for clarity.

Figure 6. Typical PL spectra of diamonds synthesized in the Mg-Si-C system at (a) 1700 °C, (b) 1800 °C and (c) 1900 °C. The spectra are normalized to the intensity of the diamond Raman peak and dispalced vertically for clarity.

Figure 7. PL spectrum of a diamond crystal from the Mg-Si-C system showing peaks at 1.682 and 1.722 eV with comparable intensities.

Figure 8. Degree of the graphite-to-diamond transformation in the Mg-Si-C and Mg-C systems as a function of the reaction time at different temperatures. Data for the Mg-C system are taken from ref. 23. Open symbols refer to experiments where no spontaneous diamond nucleation was observed.

Figure 9. SEM micrographs of an octahedral diamond crystal with stepped surface structure: (a) general view, (b, c) fragments of the {111} face with growth pyramids.

Figure 10. SEM micrographs of diamond with carbides: (a) intergrowth of diamond octahedrons and SiC tetrahedrons; (b) SiC tetrahedrons on the stepped {111} surfaces of diamond; (c) microspheres of the $(Si_{0.75}Mg_{025})C_2$ carbide on the diamond surface. The micrographs are taken in the backscattered electrons mode.

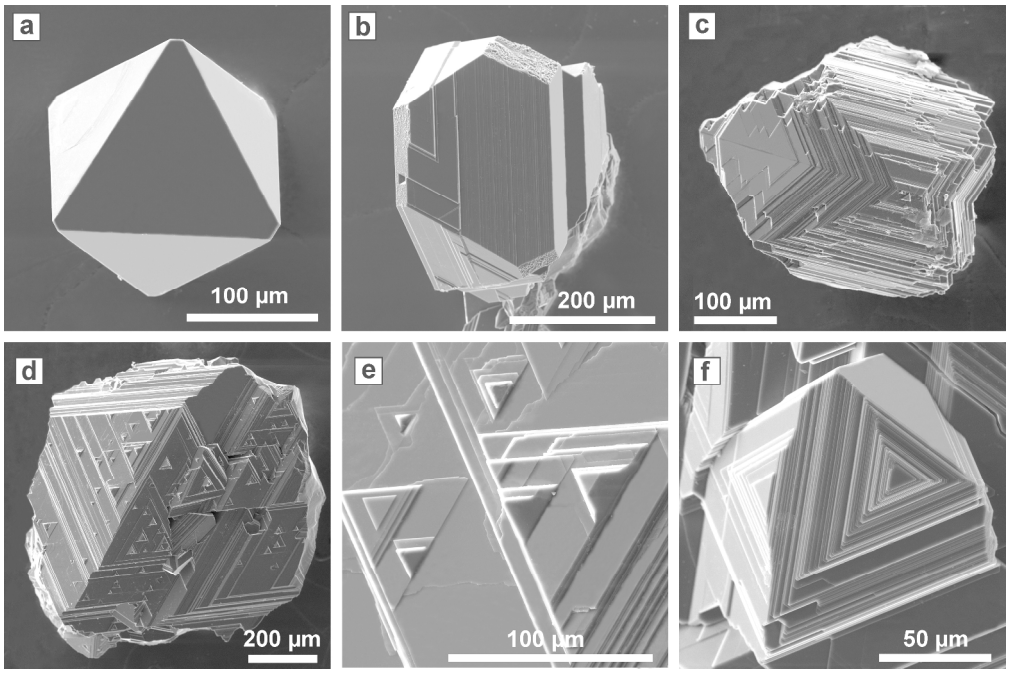

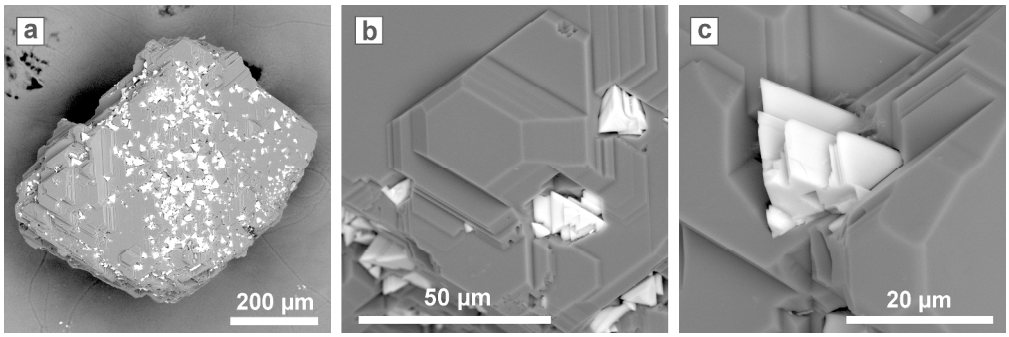

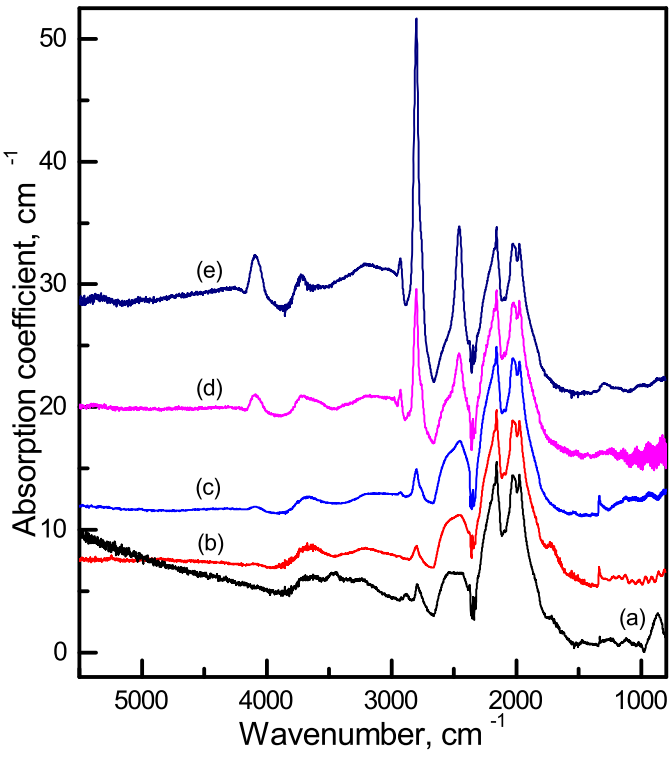

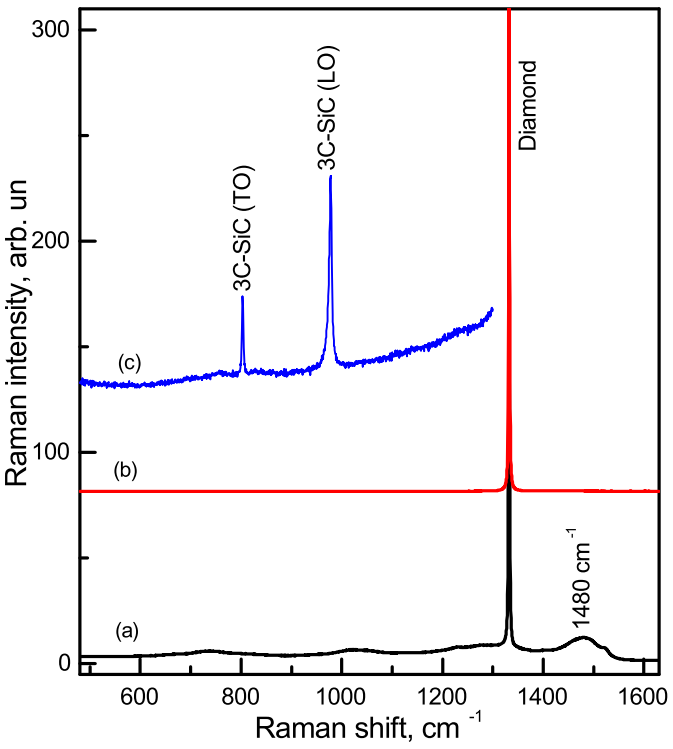

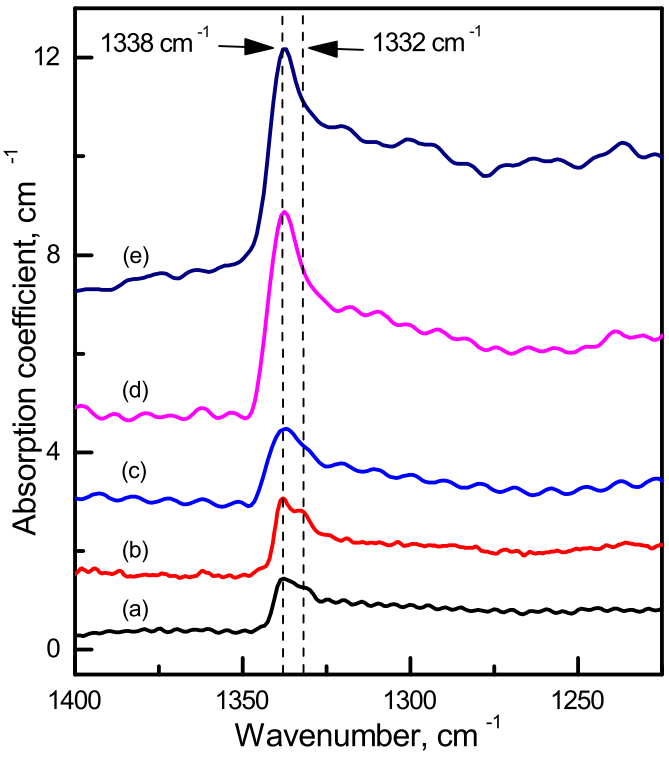

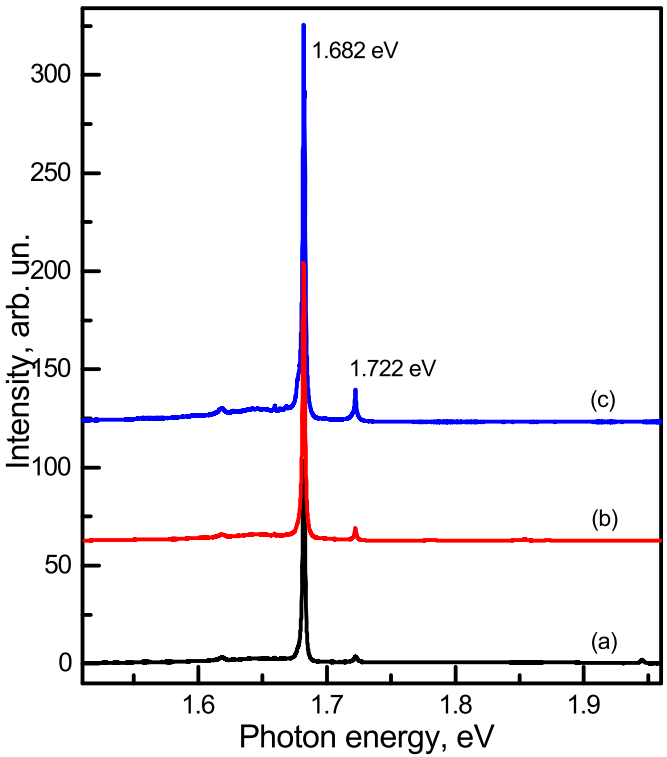

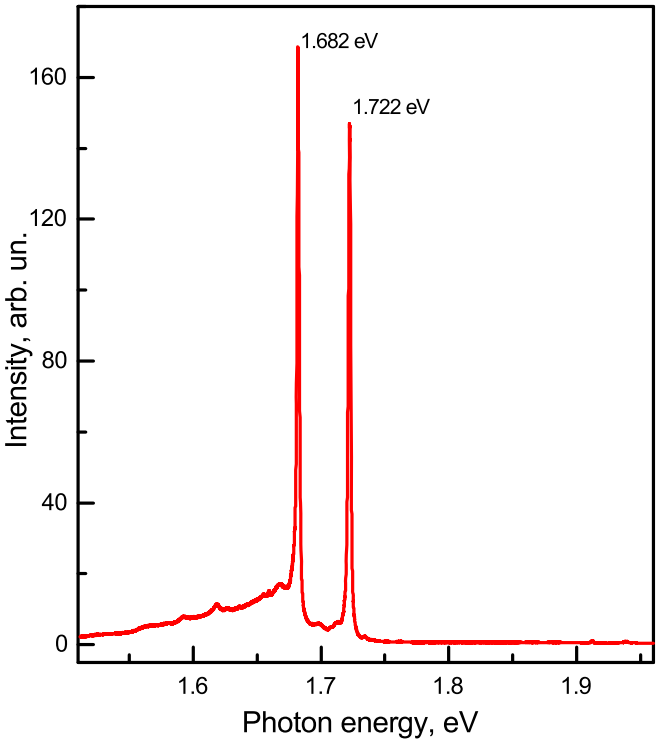

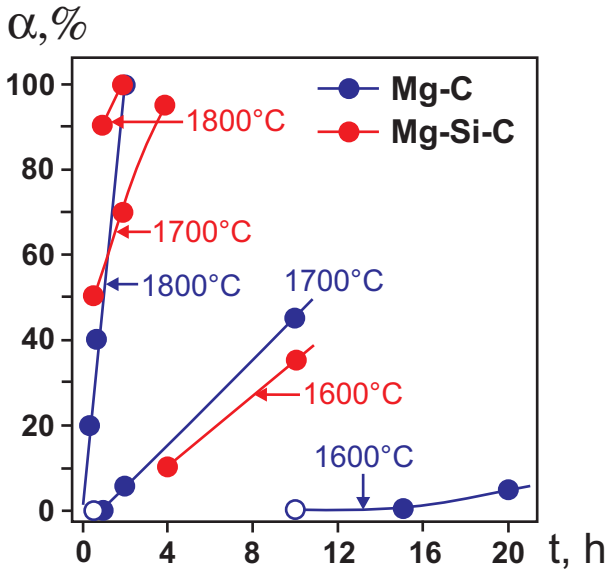

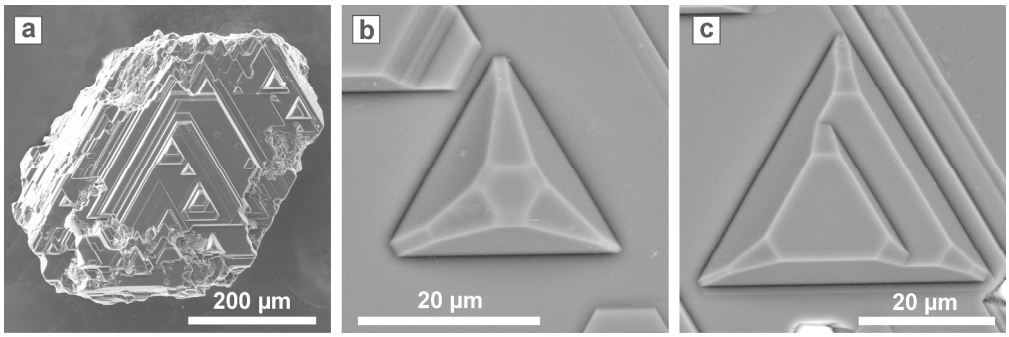

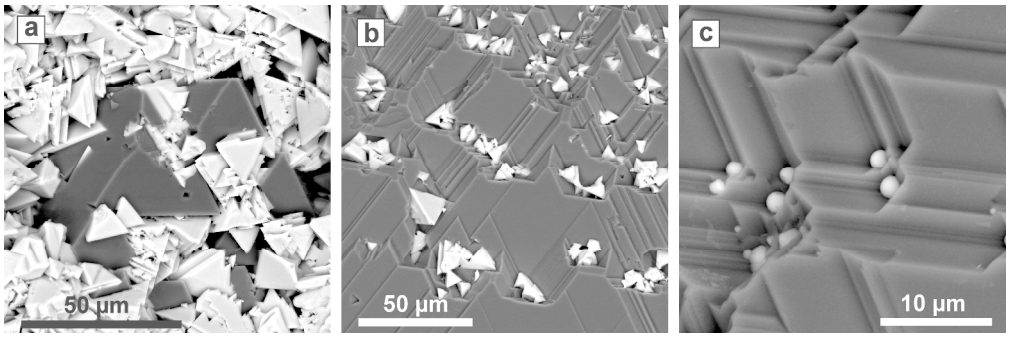

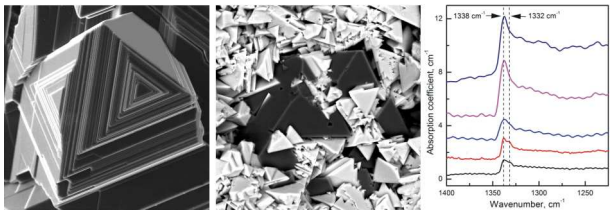

High pressure synthesis of silicon doped diamond from the Mg-Si-C system is demonstrated. The effects of Si on crystallization and spectroscopic characteristics of diamond are established.